Digital Object Identifier (DOI): 10.1109/IECON.2016.7793075

42nd Annual Conference of the IEEE Industrial Electronics Society, Florence, Italy, 2016

Resonance identification and damping in AC-grids by means of multi MW grid converters

Lars Jessen
Zhi-Xiang Zou
Berthold Benkendorff
Marco Liserre
Friedrich W. Fuchs

Suggested Citation

L. Jessen, Z. Zou, B. Benkendorff, M. Liserre and F. W. Fuchs, "Resonance identification and damping in AC-grids by means of multi MW grid converters," 42nd Annual Conference of the IEEE Industrial Electronics Society (IECON), Florence, 2016, pp. 3762-3768.

Resonance Identification and Damping in AC–Grids by Means of Multi MW Grid Converters

Lars Jessen, Zhixiang Zou, Berthold Benkendorff, Marco Liserre and Friedrich W. Fuchs
Chair of Power Electronics
Christian-Albrechts-University of Kiel
Kaiserstraße 2, 24143 Kiel, Germany
Email: {lje, zz, bb, ml, fwf}@tf.uni-kiel.de

***Abstract*—The massive integration of decentralized energy resources (DERs) poses a big challenge on the grid management. The resulting problems often require advanced power electronics based solutions like active filters or STATCOMs or even more futuristic system level solutions like smart transformers. The interaction of all the mentioned systems through grid connected converters originate stability problems. The identification of the system impedance or directly of the possible resonance and the consequent implementation of flexible and tunable damping solutions like notch filters, is discussed in this paper with reference to an already present measurement campaign. The results of an already developed 1 MVA power converter are shown. Meanwhile, a project is carrying to realize a multi megawatt medium voltage grid impedance analyzer. In this paper different scenarios are analyzed in simulation and experimentally.**

I. Introduction

The performance of electrical grids is changing considerably due to the steadily growing integration of decentralized energy resources (DERs), such as power generation from wind or solar energy. Besides the feed–in of active and reactive power, the DERs introduce not only additional filter elements, such as inductors and capacitors, that are influencing the grid impedance, also when the DERs are not injecting power, but also fast controllers and synchronization systems which influence the impedance of DERs [1] and as a consequence the overall system impedance. The knowledge of the grid impedance is of high importance for the generation and limitation of harmonics, for setting voltage harmonic limitations in grid standards, and for the design of grid connected power converters. Moreover, the control of the power converters of DERs has to be adapted to the grid impedance to guarantee stability and sufficient dynamic behavior.

In the conventional approach for the grid connection of DERs, the grid impedance at the point of connection (PoC) is calculated at the fundamental grid frequency based on short circuit power [2]. In special cases grid simulation software is used to obtain more precise results. Nevertheless, this approach is insufficient since the grid impedance between $0.1\,\mathrm{kHz}$ and $10\,\mathrm{kHz}$, the range of the dominant harmonic frequencies of the DERs, has to be known. This is valid for both low–voltage (LV) grids with smaller DERs and medium–voltage (MV) grids, where wind and solar parks are connected, for instance. For LV grids, some measurements of the performance of the grid impedance in the interesting frequency range of $0.1\,\mathrm{kHz}$ to $10\,\mathrm{kHz}$ under varying grid conditions are published [3], [4], [5]. It is possible to foresee that in a future more dynamic grid where more grid–converters are frequently connected and disconnected leading to variable impedance situation. Hence, it will be mandatory that the existing grid–converters and/or extra system measure the grid impedance and are able to provide power system damping. This paper attempts to give an overall analysis based on existing grid impedance measurement methods and proposes tailored active damping solutions which could be implemented in large hardware systems like a $1\,\mathrm{MVA}$ NPC converter which results are reported in the present digest. This paper is organized as follows: Section II introduces the problem of resonance identification in AC grids in case of different scenarios and gives more details for a specific case. In Section III the use of notch filter for active damping of different resonances is introduced. Additionally, the flexibility of this method is shown. This is validated by simulations in section IV. In Section V results from resonance identification with already existing hardware is presented. Tests with a $1\,\mathrm{MVA}$ NPC converter as preparation for building a multi megawatt power converter are shown in section VI.

II. Resonance Identification

Several methods for grid resonance identification by grid impedance measurement have been published [2], [3], [4], [6]. Mostly, grid impedance measurements are carried out either by monofrequent current injection [4], [7] or polyfrequent current injection [8], [9]. These systems are often designed exclusively for measuring purpose and hence, are dedicated only for grid impedance measurements. Anyway, there are also approaches to integrate monofrequent and polyfrequent grid impedance measurement methods in already existing solar or wind power inverters as STATCOM or smart transformers [10], [11] [12] and [13], fig. 1. However, in most cases these systems aim at detecting the grid impedance at fundamental frequency for adapting converter control to shifting LCL filter resonance due to changing grid impedances.

In this paper the grid impedance is measured by monofrequent current injection in a wide frequency range from $80\,\mathrm{Hz}$ to $10\,\mathrm{kHz}$. The measurement procedure is as follows. First, a certain current of a specific frequency is injected into the grid by a monofrequent current generator. Then the voltage

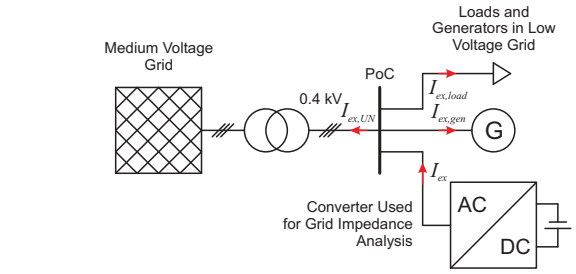

(a)

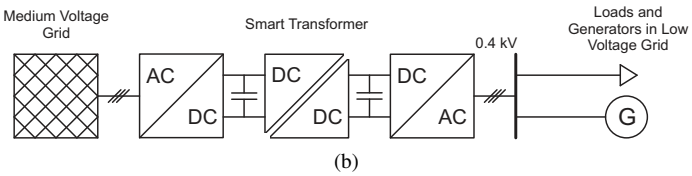

(b)

Fig. 1. Resonance identification by means of a parallel (a) or series (b) grid connected converter.

of the grid at the point of connection is measured. After that, magnitude and phase angle of voltage and current at the desired frequency are determined by FFT. With this harmonic spectrum, the grid impedance can be calculated according to Ohm's law. This procedure is repeated at all required frequencies.

$$\underline{Z}_{PoC}(f) = \frac{\underline{V}_{PoC}(f)}{\underline{I}_{ex}(f)} \tag{1}$$

Considering the setup in fig. 1a it is also possible to measure the impedance of each connection on the busbar PoC due to current divider by

$$\underline{Z}_{UN}(f) = \frac{\underline{V}_{PoC}(f)}{\underline{I}_{ex,UN}(f)} \tag{2}$$

$$\underline{Z}_{load}(f) = \frac{\underline{V}_{PoC}(f)}{\underline{I}_{ex,load}(f)} \tag{3}$$

$$\underline{Z}_{gen}(f) = \frac{\underline{V}_{PoC}(f)}{\underline{I}_{ex,gen}(f)} \tag{4}$$

and calculate the impedance of the PoC by parallel connection of these impedances

$$\underline{Z}_{PoC}(f) = \left(\frac{1}{\underline{Z}_{UN}(f)} + \frac{1}{\underline{Z}_{load}(f)} + \frac{1}{\underline{Z}_{gen}(f)} \right)^{-1} . \tag{5}$$

Therefore, this setup allows determination of the grid impedance as well as disposition of the contribution of each connection to $\underline{Z}_{PoC}(f)$.

A combination of an inverter with the output impedance $\underline{Z}_o$ and a PoC in the grid with the impedance $\underline{Z}_{PoC}$ can be represented by the equivalent circuit depicted in fig. 2. In this system the stability can be determined by analyzing $\underline{Z}_{PoC}\underline{Y}_o$ in accordance to [14], [15]. However, to achieve a stable operation in the presence of grid resonances proper

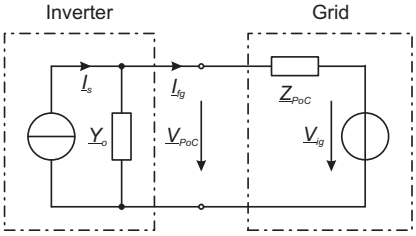

Fig. 2. Equivalent network of a grid connected inverter for small signal analysis.

active damping of the converter might become necessary. This challenge is focused in section III.

In the following, a dedicated system for grid impedance analysis and resonance identification is shown. This system consists of a hysteresis current controlled voltage source inverter which is illustrated in fig. 3a, [16], [17]. With this system the grid impedance can be measured in a wide frequency range from 80 Hz to 10 kHz with high accuracy. The excitation current generator system consists of a three-phase two level voltage source inverter (VSI), a 3–phase L filter and a step up transformer to achieve the necessary voltage to feed in the measurement currents into the low voltage grid, see fig. 3a. For that also a PLL is necessary. With this system an excitation of the grid with maximum current of 20 A is possible. Fig. 3b illustrates the converter output current while injecting a hysteresis controlled current at 2 kHz to measure the grid impedance. This setup is used to analyze grid resonances for robust control of a grid connected converter connected to a grid impedance containing resonances.

III. Notch Filter Active Damping

In order to well damp the grid resonance identified in Section II, a filter–based active damping can be incorporated with the current controller to reshape the impedance characteristics in an AC grid. Several filter–based active damping methods have been proposed in literature for performance improvement of grid converters with LCL–filter [18]. Among these methods, Notch Filter (NF) based active damping is one of the most promising alternatives to mitigate the resonance of AC grids and give advantages in terms of easy implementation and good robustness [11]. The main idea of NF-based active damping is to generate an negative resonant peak at grid resonant frequency as a consequence to largely alleviate grid resonance. The generic transfer function of a NF is shown as

$$N(s) = \frac{s^2 + 2D_z\omega_{nf}s + \omega_{nf}^2}{s^2 + 2D_p\omega_{nf}s + \omega_{nf}^2} \tag{6}$$

where ω_{nf} is the notch frequency, D_z and D_p are the damping coefficients for the zeros and poles. To well damp the resonance, the notch frequency is thereby set as $\omega_{nf} = \omega_{res}$, where ω_{res} is the resonance frequency of AC grids. The deepness of NF attenuation in this case is determined by the magnitude of grid resonance. In order to fully attenuate the identified resonant peak, the total equivalent admittance (PoC

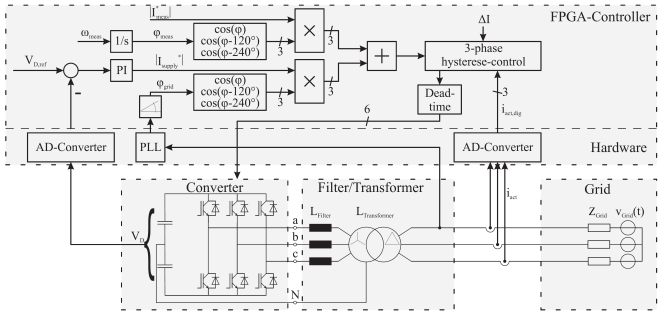

(a)

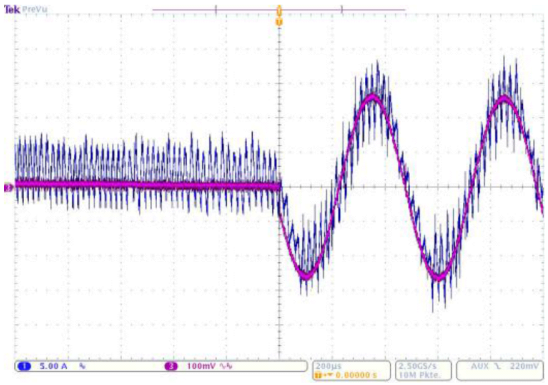

(b)

Fig. 3. (a) Control design of the high frequency measurement current generator. (b) Hysteresis controlled current for grid impedance measurement at 2 kHz, CH1: Injected current (dark blue), CH2: Reference current (purple)

admittance $Y_{PoC} = 1/Z_{PoC}$ and converter output admittance Y_o) after NF compensation should be positive (> 0 dBS). Here, Y_o represents the output admittance of a grid-tied converter, whose expression is given by [15]

$$Y_o = \frac{I_g}{V_{PoC}} = \frac{G_d G_f}{1 + N G_c G_d G_f} \tag{7}$$

where G_c, G_d, and G_f are the transfer functions of the current controller, the computation and PWM delays, and the output filter, respectively. $G_{op} = G_c G_d G_f$ is the open-loop transfer function of the original control system without NF damping. Note that the output admittance can be easily modified by either the current controller or the filters in feed-forward channel [19]. The NF appeared in the denominator is basically suitable for shaping independently of the grid converter admittance to deal with resonance issues.

As a consequence, the total admittance seen from the PoC at ω_{res} could be reduced. The expression of the total admittance is given by

$$\begin{aligned} Y_{total}(s) &= |Y_{PoC}(s) + Y_o(s)|_{s=j\omega_{res}} \\ &= \left| Y_{PoC}(s) + \frac{G_d(s) G_f(s)}{1 + G_{op}(s) N(s)} \right|_{s=j\omega_{res}} \\ &\geq 1 \end{aligned} \tag{8}$$

Since the amplitudes of $Y_{PoC}(s)$ and $Y_o(s)$ are positive, the relationship between D_z and D_p are

$$\begin{aligned} \frac{D_z}{D_p} &= |N(s)|_{s=j\omega_{res}} \\ &< \left(\frac{|G_d(s) G_f(s)|}{1 - |Y_{PoC}(s)|} - 1 \right) |G_{op}(s)|^{-1} |_{s=j\omega_{res}} \end{aligned} \tag{9}$$

In digital NF design, $D_z = 0$ is commonly used to obtain a significant deepness at resonant frequency and it can fulfill the condition of (9) as well.

It is worth noting that the NF introduces phase lag below the notch frequency which is likely to decrease the phase margin of the original system. The frequency response of NF within this frequency range can be written as

$$N(j\omega) = \frac{(\omega_{nf}^2 - \omega^2)}{(\omega_{nf}^2 - \omega^2) + j2D_p\omega_{nf}\omega} \tag{10}$$

and the phase angle of (10) can be obtained as

$$\angle N(j\omega) = -\arctan \frac{2\omega_{nf}\omega D_p}{\omega_{nf}^2 - \omega^2} \tag{11}$$

To achieve a high stability margin for the grid converter, the phase margin of the overall system should maintain as

$$45^\circ \leq \angle PM + \angle N(j\omega_c) \leq 60^\circ \tag{12}$$

where ω_c is the cut-off frequency of the original system G_{op}.

Hence, D_p can be tuned to fulfill stability condition of (12). On the other hand, in a practical AC grid, the fundamental frequency is not fixed and therefore the resonance frequency varies in a certain range with the changing fundamental frequency. With this consideration, a wide bandwidth NF is required to enhance the robustness of the system and reduce its sensitivity to the frequency. According to the NF characteristics, the bandwidth of NF is determined by D_p as well. It can be seen that the NF bandwidth increases by increasing of D_p but at the same time the phase margin reduces. Therefore, a tradeoff must be made between stability and robustness of the overall system.

The analysis of the open-loop Bode plot using NF active damping is shown in Fig. 4. For comparison, the original system along with grid resonance is shown as red curves, where the resonant frequency is 2860 Hz. To compensate the peak of resonance, an NF with same notch frequency and bandwidth of 1450 Hz is designed. It is obviously seen that the grid resonance has been well damped. Moreover, the stability of the overall system has been improved since there is no -180° crossing when the magnitude is positive. The root locus of the undamped system as well as the NF-damped system has been shown in Fig. 5. It is can be seen that the poles located on the unity cycle due to the resonance can be canceled by the zeros introduced by the NF active damping.

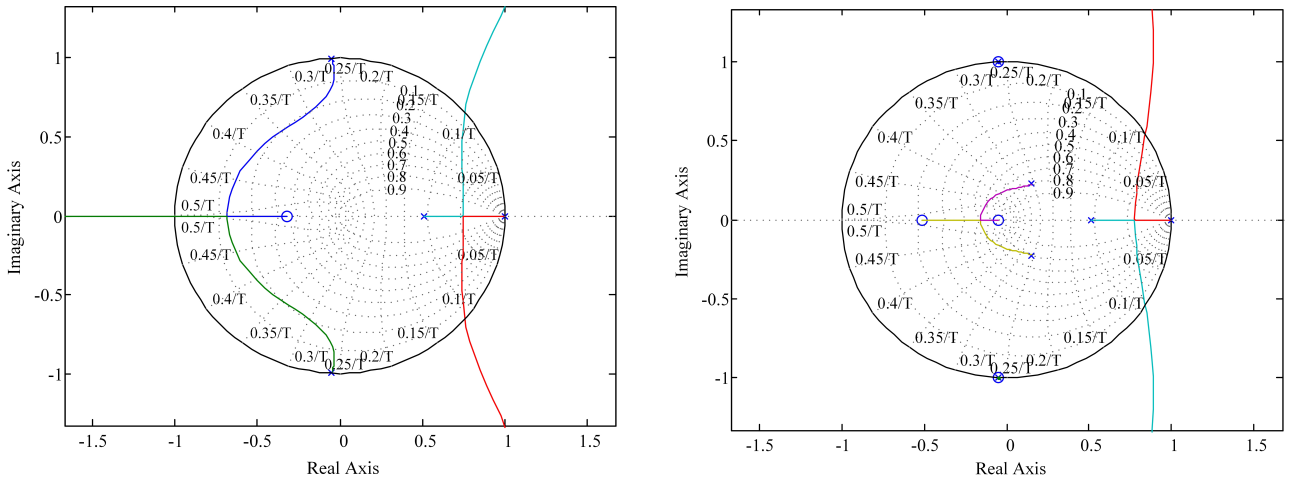

(a) (b)

Fig. 5. Root locus of (a) undamped system and (b) NF-damped system.

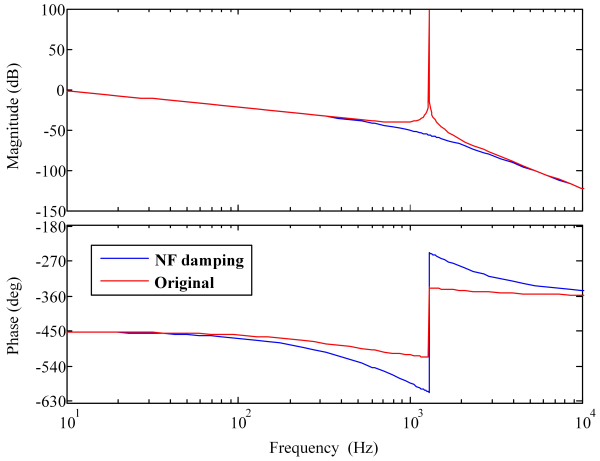

Fig. 4. Open-loop Bode diagrams of the current-controlled grid-tie converter (red curves) and with an NF active damping (blue curves).

IV. Simulation Results

The NF damping effect for the grid resonance has been tested in simulation. The results are depicted in fig. 6a. The NF is implemented into the grid converter at $t = 0.3\,\mathrm{s}$ when the grid resonance has been identified. It is clearly seen that the NF active damping can well stabilize system and mitigate the current oscillation caused by the grid resonance. In figure 6b, the robustness of the NF damping method has been studied, in which the deviation between the identified grid impedance and the actual grid impedance is 0.5 p.u. The NF active damping with two different bandwidth are implemented in the grid converter. The NF bandwidth increases from 500 Hz to 1450 Hz at $t = 0.3\,\mathrm{s}$ and the result shows that the current becomes more robust when a higher bandwidth NF is used.

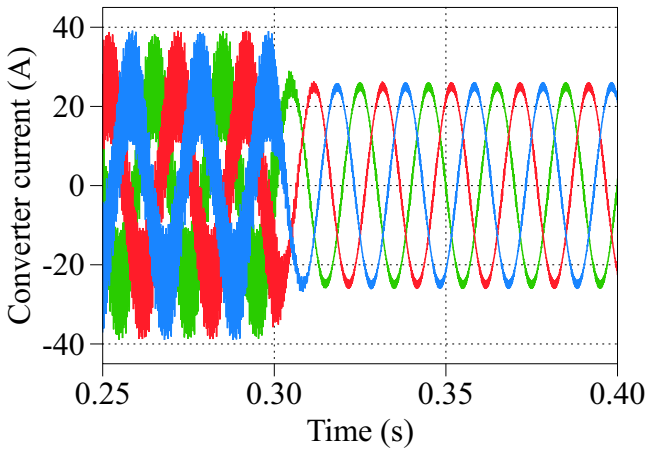

(a)

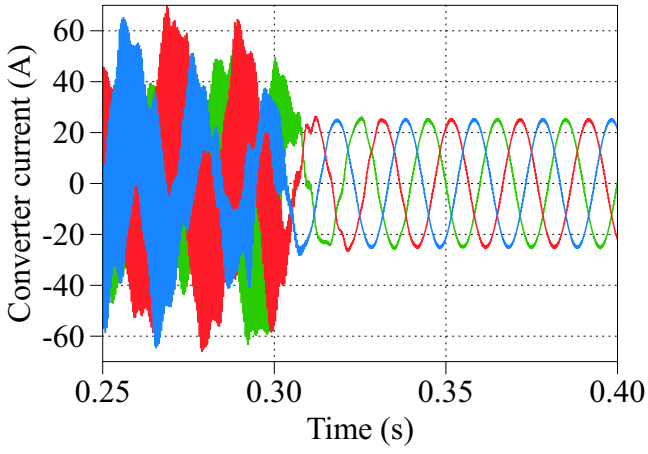

(b)

Fig. 6. Effect of NF active damping on grid converter current: (a) resonance damping and (b) robustness study.

V. Results From Low Voltage Grid Impedance Measurements

In this section long term grid impedance measurements recorded by the measurement system described in section II are presented [20]. The measurements are performed in a public low voltage distribution grid in northern Germany. This grid contains 49 private household customers and 14 solar power plants witch are operated by grid customers. The total peak power of of the solar power plants is about 164 kVA. The grid is connected to the upstream medium voltage gird by a 400 kVA transformer. In agreement with the distribution system operator the structure of the low voltage grid remains unchanged during the measurements.

The grid impedance is measured continuously every half hour for 96 hours from Friday noon to Tuesday noon. Fig. 7a depicts the magnitude of the impedance of the PoC $\underline{Z}_{PoC}(f)$. It can be seen that the frequency depending impedance of the PoC varies in time with a clear day and night profile. Furthermore, several resonances can be found, fig. 7a. The most significant resonance occurs at 1.8 kHz with a magnitude of $Z_{PoC} = 1.3\,\Omega$. It shows up between 10:30 p.m. and 5:30 a.m.

Fig. 7b shows the time dependency of $\underline{Z}_{PoC}$ for four different frequencies in comparison to the approximated grid impedance $\underline{Z}_{apx}$. The approximated grid impedance is based on short circuit network calculation which provides a short circuit power and a short circuit angle at 50 Hz. With this information and the resistive–inductive model of the power system the grid impedance can be approximated by $\underline{Z}_{apx}(\omega) = R_{apx} + \mathrm{j}\omega L_{apx}$ where $R_{apx} = 64.2\,\mathrm{m}\Omega$ and $L_{apx} = 77.9\,\mu\mathrm{H}$.

The comparison of $\underline{Z}_{apx}$ and $\underline{Z}_{PoC}$ shows that at 0.25 kHz both impedances are more or less equal. At 1.8 kHz the resonance results in an actual impedance that is smaller than Z_{apx} during daytime and larger than Z_{apx} during nighttime. At higher frequencies like 3.3 kHz a great difference between $\underline{Z}_{apx}$ and $\underline{Z}_{PoC}$ arises. In addition, it can be noticed that the grid impedance magnitude at 3.3 kHz is always smaller in comparison to 1.8 kHz and usually smaller in comparison to 1 kHz. This can be explained by the variable ohmic, inductive and capacitive power system elements that form the impedance of the PoC.

Another interesting aspect when regarding the grid impedance is the daily repeating pattern. This pattern can be investigated by partitioning the data on a daily basis and calculating the arithmetic mean as well as the standard deviation at each half hour a day by

$$\bar{x} = \frac{1}{n}\sum_{i=1}^{n} x_i \tag{13}$$

$$std = \sqrt{\frac{1}{n-1}\sum_{i=1}^{n}(x_i - \bar{x})^2} \tag{14}$$

where $n = 4$. Fig. 7c illustrates that the change in impedance for a specific time instant at different days is

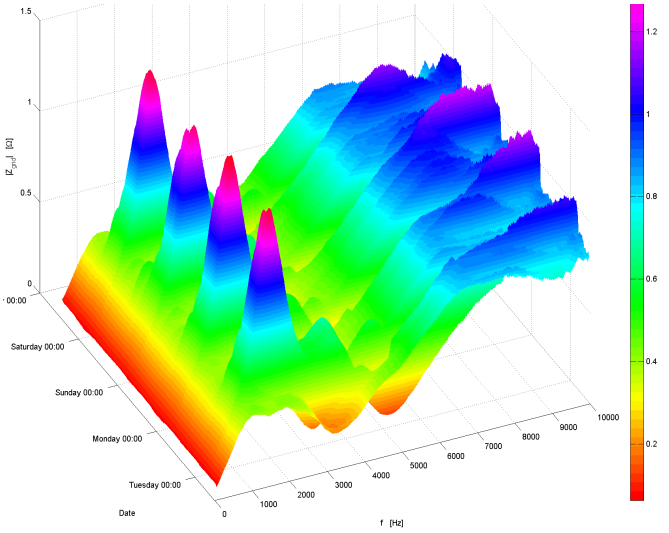

(a)

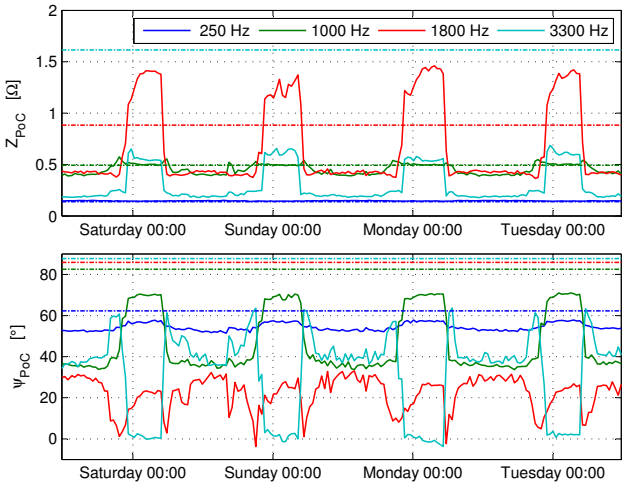

(b)

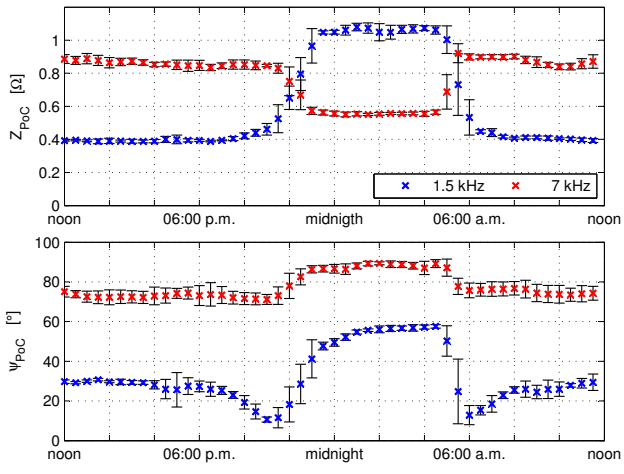

(c)

Fig. 7. (a) Grid impedance magnitude versus time and frequency in a public low voltage distribution grid, (b) grid impedance versus time at 0.25 kHz, 1 kHz, 1.8 kHz and 3.3 kHz (solid lines indicate grid impedance measurements, dash–dotted lines indicate approximated grid impedances), (c) grid impedance arithmetic mean at 1.5 kHz and 7 kHz every half hour calculated from four days of grid impedance measurement (error bars indicate standard deviation).

rather small during daytime as well as during nighttime. Nevertheless, it can be noticed that during transition from day to night and from night to day increased standard deviations occur.

VI. Realization of a Multi–MW Converter for Grid Analysis and Damping

The results in section V are obtained from measurements in a public low voltage grid. For the future it is planned to performed grid impedance measurements in medium voltage grids. Therefore, a multi megawatt converter is developed and constructed. This section shows results from tests with a converter at a power of approximately 1 MVA.

The multi megawatt power converter has been designed with NPC topology and a DC–link of 1.5 kV. Caused by the topology, the blocking voltage of the semiconductor has to be only 1.2 kV. This is possible because the blocking voltage of the semiconductor has only to withstand half of the DC-link voltage. Compared to an equal two level inverter, a lower RMS current, a smaller filter size and a smaller cross section of the cables are possible at the same apparent power of approximately 1 MVA. The parameters of the three level NPC Power-Stack can be found in [21].

The three level NPC converter was tested and verified in a circulation power method. This three level converter was set as a receptor. A second equal three-level inverter was not available at that time. That is why an equivalent two level inverter with similar power is taken as a generator. Both AC-sides of the two converters are connected via an three-phase inductor. Likewise both DC-links are connected, via short bus bar configuration. The DC-supply has mainly to power the losses of both converters.

For this verification setup of the inverter losses and the efficiency, six current and six voltage sensors are needed for the measurement setup. For the analysis of the total losses and the efficiency a power analyzer is used, to supervise the output voltage and current a scope recorder is applied [22]. Fig. 8 shows the experimental results at different operation points of the three level NPC inverter.

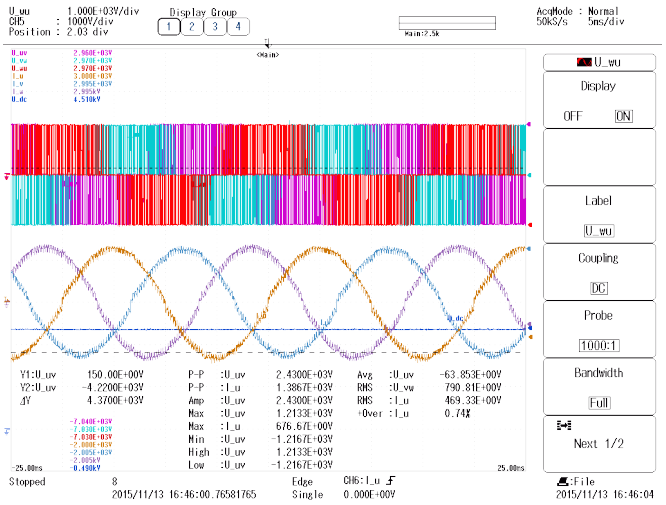

(a)

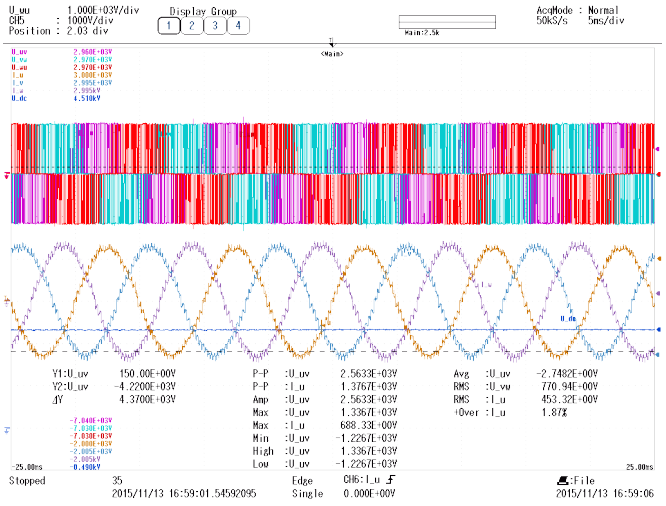

(b)

Fig. 8. Experimental results of the NPC measured AC-phase line-to-line voltage and AC-phase current ($f_{\mathrm{sw}} = 4.5\,\mathrm{kHz}$, $T_{\mathrm{a}} = 25\,^{\circ}$ for $i_{\mathrm{rms}} = 600\,\mathrm{A}$ and $m = 1$) with (a) in grid-side operation at $f_{\mathrm{N}} = 50\,\mathrm{Hz}$ with $cos\varphi \approx 1.0$ and with (b) in generator-side operation at $f_{\mathrm{N}} = 100\,\mathrm{Hz}$ with $cos\varphi \approx -1.0$ for (a),(b) with $U_{\mathrm{DC}} = 1200\,\mathrm{V}$

VII. Conclusion

The paper aims at giving an overview of grid resonance identification and damping with grid connected converters. The results of a vast measurement campaign have identified possible grid resonance problems. Furthermore, this paper shows that the impact of grid resonances on converter control performance can significantly be reduced by a notch–filter. Finally, this paper presents first steps for realizing a multi megawatt converter for medium voltage grid impedance identification and damping.

References

[1] F. Blaabjerg, Z. Chen, and S. B. Kjaer, "Power electronics as efficient interface in dispersed power generation systems," *IEEE Transactions on Power Electronics*, vol. 19, no. 5, pp. 1184–1194, 2004.

[2] M. Sumner, B. Palethorpe, and D. Thomas, "Impedance measurement for improved power quality - part 1: The measurement technique," *IEEE Transactions on Power Delivery*, vol. 19, no. 3, pp. 1442–1448, 2004.

[3] Y. A. Familiant, J. Huang, K. A. Corzine, and M. Belkhayat, "New techniques for measuring impedance characteristics of three-phase ac power systems," *IEEE Transactions on Power Electronics*, vol. 24, no. 7, pp. 1802–1810, 2009.

[4] A. Knop and F. W. Fuchs, "High frequency grid impedance analysis by current injection," *Industrial Electronics, 2009. IECON '09. 35th Annual Conference of IEEE*, pp. 536–541, 2009.

[5] S. Günter, F. W. Fuchs, and H.-J. Hinrichs, "A method to measure the network harmonic impedance," *PCIM Europe 2013, 14 – 16 May 2013, Nuremberg*, 2013.

[6] Y. L. Familiant, K. A. Corzine, J. Huang, and M. Belkhayat, "Ac impedance measurement techniques," *Electric Machines and Drives, 2005 IEEE International Conference on*, pp. 1850–1857, 2005.

[7] J. Xie, Y. X. Feng, and N. Krap, "Network impedance measurements for three-phase high-voltage power systems," *Power and Energy Engineering Conference (APPEEC), 2010 Asia-Pacific*, pp. 1–5, 2010.

[8] M. Jordan, H. Langkowski, T. D. Thanh, and D. Schulz, "Frequency dependent grid-impedance determination with pulse-width-modulation-signals," *2011 7th International Conference-Workshop Compatibility and*

Power Electronics (CPE), pp. 131–136, 2011.

[9] M. Cespedes and J. Sun, "Online grid impedance identification for adaptive control of grid-connected inverters," *IEEE Energy Conversion Congress and Exposition (ECCE)*, pp. 914–921, 2012.

[10] N. Hoffmann and F. W. Fuchs, "Online grid impedance estimation for the control of grid connected converters in inductive-resistive distributed power-networks using extended kalman-filter," *Energy Conversion Congress and Exposition (ECCE), 2012 IEEE*, pp. 922–929, 2012.

[11] R. Peña Alzola, M. Liserre, F. Blaabjerg, M. Ordonez, and T. Kerekes, "A self-commissioning notch filter for active damping in a three-phase lcl -filter-based grid-tie converter," *Power Electronics, IEEE Transactions on*, vol. 29, pp. 6754–6761, Dec 2014.

[12] A. Riccobono, Naqvi, Syed Khurram Abbas, A. Monti, T. Caldognetto, J. Siegers, and E. Santi, "Online wideband identification of single-phase ac power grid impedances using an existing grid-tied power electronic inverter," *Power Electronics for Distributed Generation Systems (PEDG), 2015 IEEE 6th International Symposium on*, pp. 1–8, 2015.

[13] D. Martin, E. Santi, and A. Barkley, "Wide bandwidth system identification of ac system impedances by applying pertubations to an existing converter," *Energy Conversion Congress and Exposition (ECCE), 2011 IEEE*, pp. 2549–2556, 2011.

[14] J. Sun, "Small-signal methods for ac distributed power systems – a review," *IEEE Transactions on Power Electronics*, vol. 24, no. 11, pp. 2545–2554, 2009.

[15] J. Sun, "Impedance-based stability criterion for grid-connected inverters," *Power Electronics, IEEE Transactions on*, vol. 26, pp. 3075–3078, Nov 2011.

[16] A. Knop and F. W. Fuchs, "High frequency grid impedance analysis with three-phase converter and fpga based tolerance band controller," *Compatibility and Power Electronics, 2009. CPE '09.*, pp. 286–291, 2009.

[17] S. Günter and F. W. Fuchs, "Switching time prediction for digital hysteresis control for high frequency current in grid impedance measurement application," *Power Electronics and Applications (EPE'14-ECCE Europe), 2014 16th European Conference on*, pp. 1–8, 2014.

[18] J. Dannehl, M. Liserre, and F. W. Fuchs, "Filter-based active damping of voltage source converters with lcl filter," *Industrial Electronics, IEEE Transactions on*, vol. 58, pp. 3623–3633, Aug 2011.

[19] Z. Zou, Z. Wang, and M. Cheng, "Modeling, Analysis, and Design of Multifunction Grid-Interfaced Inverters with Output LCL Filter," *Power Electronics, IEEE Transactions on*, vol. 29, pp. 3830–3839, July 2014.

[20] L. Jessen, S. Gunter, F. W. Fuchs, M. Gottschalk, and H.-J. Hinrichs, "Measurement results and performance analysis of the grid impedance in different low voltage grids for a wide frequency band to support grid integration of renewables," *Energy Conversion Congress and Exposition (ECCE), 2015 IEEE*, pp. 1960–1967, 2015.

[21] B. Benkendorff, F. W. Fuchs, D. Friedrich, J. Hinz, M. Poech, K. Kohlmann, H. Reese, H.-H. Letas, C. Weber, R. Eisele, Z. Mueller, M. Berger, J. Rudzki, F. Osterwald, and T. Mono, "Bottom up research and development for a low-voltage three level npc converter," in *Proceedings of PCIM Europe 2015; International Exhibition and Conference for Power Electronics, Intelligent Motion, Renewable Energy and Energy Management*, pp. 1–8, May 2015.

[22] B. Benkendorff, T.-W. Franke, and F. W. Fuchs, "Efficiency verification power circulation method of a high power low voltage npc converter for wind turbines," in *Proceedings of PCIM Europe 2016; International Exhibition and Conference for Power Electronics, Intelligent Motion, Renewable Energy and Energy Management (accepted for publication)*, pp. 1–8, May 2016.